Earth and Planetary Science Letters 410 (2015) 75–83

Contents lists available at ScienceDirect

Earth and Planetary Science Letters

www.elsevier.com/locate/epsl

Experimental constraints on the composition and dynamics of Titan's polar lakes

A. Luspay-Kuti [a,b,*], V.F. Chevrier [b], D. Cordier [c], E.G. Rivera-Valentin [d], S. Singh [b], A. Wagner [b], F.C. Wasiak [b]

[a] Space Science & Engineering Division, Southwest Research Institute, 6220 Culebra Rd., San Antonio, TX 78238, USA
[b] Arkansas Center for Space and Planetary Sciences, STON F47, 346 1/2 N. Arkansas Ave., University of Arkansas, Fayetteville, AR 72701, USA
[c] Université de Franche-Comté, Institut UTINAM, CNRS/INSU, UMR 6213, Besancon Cedex, France
[d] Arecibo Observatory (USRA), National Astronomy and Ionosphere Center, Arecibo, PR 00612, USA

ARTICLE INFO

Article history:
Received 10 December 2013
Received in revised form 4 September 2014
Accepted 4 November 2014
Available online 5 December 2014
Editor: C. Sotin

Keywords:
Titan
evaporation rate
hydrocarbon lakes
experimental
lake composition

ABSTRACT

Titan's polar lakes are thought to be predominantly composed of liquid ethane and methane; however, little is known on the ratio of these hydrocarbons in the lakes, and the stability and dynamics of these mixtures. Here we provide the first experimental constraints under Titan surface conditions of liquid hydrocarbon mixture evaporation. Our results are relevant to Titan's polar temperatures and pressures (~92 K and 1.5 bar), and cover a wide range of methane–ethane compositions. We show that evaporation is negligible for pure ethane, but increases nearly linearly with increasing methane concentration. Early dissolution of N_2 results in ternary mixtures evaporating, which is modeled by a 'hybrid' thermodynamic equilibrium approach combining Perturbed-Chain Statistical Associating Fluid Theory with a diffusion and buoyancy-driven mass flux model. The approach follows the experimental evaporation rate measurements presented in this study, and allows for the calculation of the corresponding liquid methane–ethane–nitrogen ratios. Such results along with *Cassini* inferred lake evaporation rates can be used to estimate the composition of Titan's polar liquids, and may have implications on their origin. Our results suggest that Ontario Lacus is predominantly composed of ethane (>50–80 mol%), indicating it may be a residual lake following extensive seasonal methane evaporation, and/or might be in contact with a subsurface liquid reservoir.

1. Introduction

One of the landmark discoveries of the *Cassini–Huygens* mission to date is the existence of stable liquid bodies on Titan's surface. *Cassini* Synthetic Aperture Radar (SAR) images showed several lake-like features in the north polar region of Titan (Stofan et al., 2007). RADAR microwave radiometry provided further evidence, suggesting these radar-dark features are in fact liquid filled basins with a dielectric constant consistent with an ethane–methane mixture (Janssen et al., 2009). Thus far, hundreds of these hydrocarbon lakes and seas have been identified, mainly confined to the colder and presumably more humid polar regions, with more observed lakes in the north (Aharonson et al., 2009). There is evidence for tropical liquids as well, possibly supplied by occasional heavy rainfall events (Turtle et al., 2011) and/or underground aquifers (Griffith et al., 2012).

While the lakes are thought to be dominated by ethane and methane, there is little direct evidence on the exact amount of these components in the liquid phase. Brown et al. (2008) reported on spectral features observed by the Visible and Infrared Mapping Spectrometer (VIMS) in Ontario Lacus that were interpreted as liquid ethane. Alternatively, Moriconi et al. (2010) suggest the same absorption feature might be in the region surrounding the lake, and could be associated with damp sediments of ethane, propane, methane and possibly other minor hydrocarbons, indicative of retreat due to evaporation. While the presence of ethane in Ontario Lacus does not rule out the presence of methane in the lake, direct surface detection of liquid methane is essentially impossible due to the strong atmospheric absorption of methane. There is, though, a variety of thermodynamic and geochemical models aimed at determining lake composition. Cordier et al. (2009) considered the lakes as non-ideal solutions in thermodynamic equilibrium with the atmosphere and calculated the ethane and methane mole percent to be 76–79% and 6–11%, respectively (Cordier et al., 2013b). Their model based on Regular Solution Theory predicts negligible amounts (~0.4–0.6%) of dissolved nitrogen in the mixture.

* Corresponding author.
E-mail address: aluspaykuti@swri.edu (A. Luspay-Kuti).

http://dx.doi.org/10.1016/j.epsl.2014.11.023
0012-821X/

Glein and Shock (2013) estimate 15.5% ethane, 68.1% methane, and 14.8% N_2 in their modified van Laar model, while Tan et al. (2013) calculate 53.2-8.3% C_2H_6, 31.8–68.4% CH_4, and 6.9–22% N_2 for the equator and poles, respectively. The discrepancy in the various model results may be due to the absence of extended datasets at Titan relevant cryogenic temperatures and pressures.

Because methane is thought to be the primary participant in the hydrological cycle on Titan (Lunine and Atreya, 2008), accurate evaporation rates are crucial for general circulation models, as well as to predict the stability of polar lakes. Luspay-Kuti et al. (2012) reported an average evaporation flux of $(3.1 \pm 0.6) \times 10^{-4}$ kg m^{-2} s^{-1} from experimental simulations for pure CH_4 in a N_2 atmosphere, with a gravity-corrected value for Titan of $(1.6 \pm 0.3) \times 10^{-4}$ kg s^{-1}m^{-2} for ∼94 K, 1.5 bar, and $\sim 2 \times 10^{-2}$ CH_4 mole fraction in the simulated atmosphere. While that study focused on evaporation of methane at equatorial temperature conditions, it does not directly represent the poles in composition.

Here we present experimental measurements on the evaporation rate of two major components of the polar lakes under Titan relevant temperature and pressure conditions for a variety of methane–ethane compositions. We also propose a model to describe mixture evaporation and liquid composition, and discuss the implications of our experimental results to Titan's lakes.

2. Laboratory simulations

We used an experimental facility specifically designed for simulating Titan surface conditions (Wasiak et al., 2013). It consists of a larger, stainless steel host chamber (Andromeda), with a smaller unit (Temperature Control Box (TCB)) located inside. Temperatures relevant to Titan are reproduced via liquid nitrogen flow through coils positioned on both the inside and outside of the TCB and within the condenser, while a 1.5 bar atmosphere is maintained with pressurized N_2. A schematic of the chamber is shown in Fig. 1.

The same simulation chamber has been used to measure pure CH_4 evaporation rates in a N_2 atmosphere with ∼20% methane relative humidity (Luspay-Kuti et al., 2012). As a continuation of that work, before simulating CH_4–C_2H_6 mixtures we ran controlled experiments on pure C_2H_6 as follows: once the required temperature and pressure conditions were achieved, we introduced ethane gas into the condenser, maintained at ∼110 K, then poured the condensed liquid into a Petri dish connected to a scale with a readability of 0.01 g. Mass loss over time was then recorded for the determination of the evaporation rate of ethane. For simulating mixtures of methane and ethane, the previous step is followed by introducing methane on top of ethane once the temperature in the condenser reaches ∼95 K. Using gas injection times and fluxes, we can control liquid masses of these different hydrocarbons based on the desired concentrations to be simulated. The samples are then allowed to mix without being stirred. The liquid and gas temperatures were measured via K type thermocouples placed at the bottom of the Petri dish, and 1 inch above it, respectively. While the chamber used in the current study was the same facility described in Luspay-Kuti et al. (2012), some experimental details, such as the cooling procedure via liquid N_2, were slightly modified, which can result in an overall higher methane relative humidity compared to the conditions in Luspay-Kuti et al. (2012).

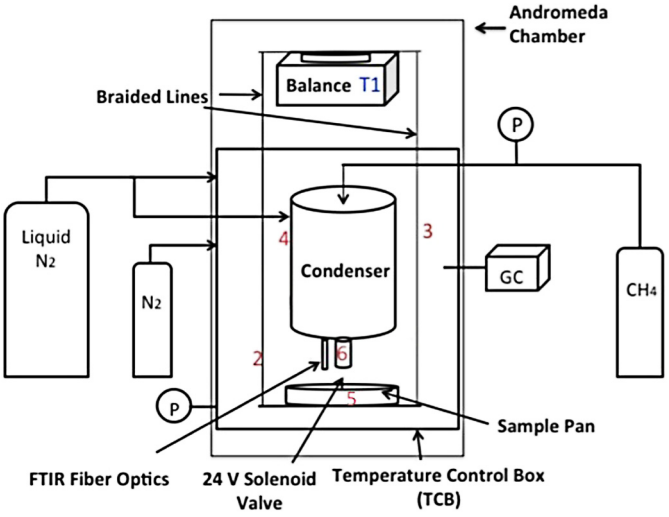

Fig. 1. Schematic diagram of the Titan simulation facility and its various components. The locations of the thermocouples are indicated with numbers. Image modified from Luspay-Kuti et al. (2012), Wasiak et al. (2013).

3. Experimental evaporation rates

The results and details for each simulation performed are summarized in Table 1. Figs. 2 and 3 show typical experimental data

Table 1
Experimentally determined evaporation rates of mixtures with various initial liquid methane mole fractions ($x_{CH_4,ini}$(exp)). The temperature values are averaged over the duration of evaporation for each individual run. The gas temperature of the simulated atmosphere was measured an inch above the liquid layer (thermocouple #2 in Fig. 1), and the temperature of the liquid was taken in the bottom of the Petri dish (thermocouple #5 in Fig. 1).

CH_4 mole fraction	Evaporation rate $\times 10^{-4}$ (kg m^{-2} s^{-1})	Standard error $\times 10^{-5}$ (kg m^{-2} s^{-1})	Average gas temperature (K)	Average liquid temperature (K)	CH_4 relative humidity	Duration of 'plateau' (s)
0.21	0.339	0.179	92.7 ± 0.3	93.4 ± 0.6	17%	n/a
0.23	0.282	0.049	91.9 ± 3.8	93.3 ± 2.3	20%	n/a
0.33	0.395	1.011	93.6 ± 1.4	95.8 ± 1.6	25%	n/a
0.44	0.621	0.199	93.3 ± 0.9	92.9 ± 0.5	25%	n/a
0.46	0.734	0.08	93.6 ± 0.7	92.9 ± 0.6	25%	n/a
0.49	0.621	0.294	93 ± 0.1	91.8 ± 0.2	28%	n/a
0.51	0.96	0.092	93.6 ± 0.4	91.6 ± 0.1	30%	n/a
0.53	1.243	0.207	92.4 ± 1.6	91.1 ± 0.9	30%	n/a
0.53	1.13	1.489	91.5 ± 0.3	90.9 ± 0.8	28%	n/a
0.63	1.525	0.233	89.7 ± 0.6	86.5 ± 0.1	30%	n/a
0.66	1.017	0.19	94.2 ± 0.6	n/a	28%	n/a
0.68	0.791	0.033	93.6 ± 2.7	92 ± 1.5	30%	n/a
0.68	1.412	0.116	90.8 ± 0.2	n/a	35%	n/a
0.74	1.243	0.187	90.9 ± 0.1	90.5 ± 0.2	33%	580
0.8	1.525	0.07	94.45 ± 0.2	92.9 ± 0.1	33%	840
0.85	2.034	0.047	91.9 ± 0.3	90.5 ± 0.6	35%	1100
0.86	1.921	0.06	93.7 ± 3.2	89.8 ± 0.8	40%	1560
0.86	1.469	0.047	n/a	n/a	39%	1700